


Fast pyrolysis bio-oil from lignocellulosic biomass for the development of bio-based cyanate esters and cross-linked networks

2019, Vol. 31(9-10) 1140–1152^a
The Author(s) 2019
Article reuse guidelines:
sagepub.com/journals-
permissions DOI:
10.1177/0954008319829517
journals.sagepub.com/home/hip



Mehul Barde^{1,2}, Charles Warren Edmunds³,
Nicole Labbe³ and Maria Lujan Auad^{1,2} 

High
Performance
Polymers



Original Article

Abstract

High Performance Polymers

Fast pyrolysis of pine wood was carried out to yield a liquid bio-oil mixture that was separated into organic and aqueous phases. The organic phase (ORG-bio-oil) was characterized by gas chromatography–mass spectroscopy, ³¹P-nuclear magnetic resonance spectroscopy, and Fourier transform infrared (FTIR) spectroscopy. It was further used as a raw material for producing a mixture of biphenolic compounds (ORG-biphenol). ORG-bio-oil, ORG-biphenol, and bisphenol A were reacted with cyanogen bromide to yield cyanate ester monomers. Cyanate esters were characterized using FTIR spectroscopy and were thermally cross-linked to develop thermoset materials. Thermomechanical properties of crosslinked cyanate esters were assessed using dynamic mechanical analysis and compared with those of cross-linked bisphenol-A-based cyanate ester. ORG-biphenol cyanate ester was observed to have a superior glass transition temperature (350–380C) as compared to bisphenol-A cyanate ester (190–220C). Cyanate esters derived from bio-oil have the potential to be a sustainable alternative to the bisphenol-A-derived analog.

Keywords

Pyrolysis, lignocellulosic biomass, bio-oil, cyanate ester, high glass transition temperature

Introduction

Cyanate esters are a class of thermoset polymeric materials that have contributed to deliver high performance in the material sciences. With unique properties such as high glass transition temperature and modulus, radar transparency, low dielectric constant and moisture absorption, high adhesion to metals, and resistance to ionizing radiation, cyanate esters are suitable materials for a wide range of applications including aerospace and microwavetransparent composites, electronic substrates, adhesives, coatings, radomes, and photonics.^{1–5} Cyanate ester monomers are cross-linked with or without catalysts at elevated temperatures to yield cross-linked networks. The crosslinking agents are not required unlike conventional thermosets such as epoxides and polyurethanes as bifunctional and multifunctional cyanate esters can self-cross-link. Nonetheless, they can be co-cross-linked with epoxides,^{6–8} benzoxazines,^{9–12} and bismaleimides,^{13,14} thereby expanding the opportunities of having versatility in the network structures and properties. As far as the performance is concerned, polycyanated materials have surpassed many thermosetting polymers and thus have intrigued polymer

chemists to continue developing cyanate ester-based materials.¹⁵ Several high-performance materials have been commercialized belonging to cyanate ester chemistry and have been used in specialty applications.² Phenol and its derivatives, especially bisphenol-A and its further modifications, have been important

1

Center for Polymers and Advanced Composites, Auburn University, Auburn, Alabama, USA

2

Department of Chemical Engineering, Auburn University, Auburn, Alabama, USA

3

Center for Renewable Carbon, University of Tennessee, Knoxville, Tennessee, USA

Corresponding author:

Maria Lujan Auad, Center for Polymers and Advanced Composites, Department of Chemical Engineering, Auburn University, Auburn, Ross Hall, 36849, Alabama, USA. Email: auad@auburn.edu

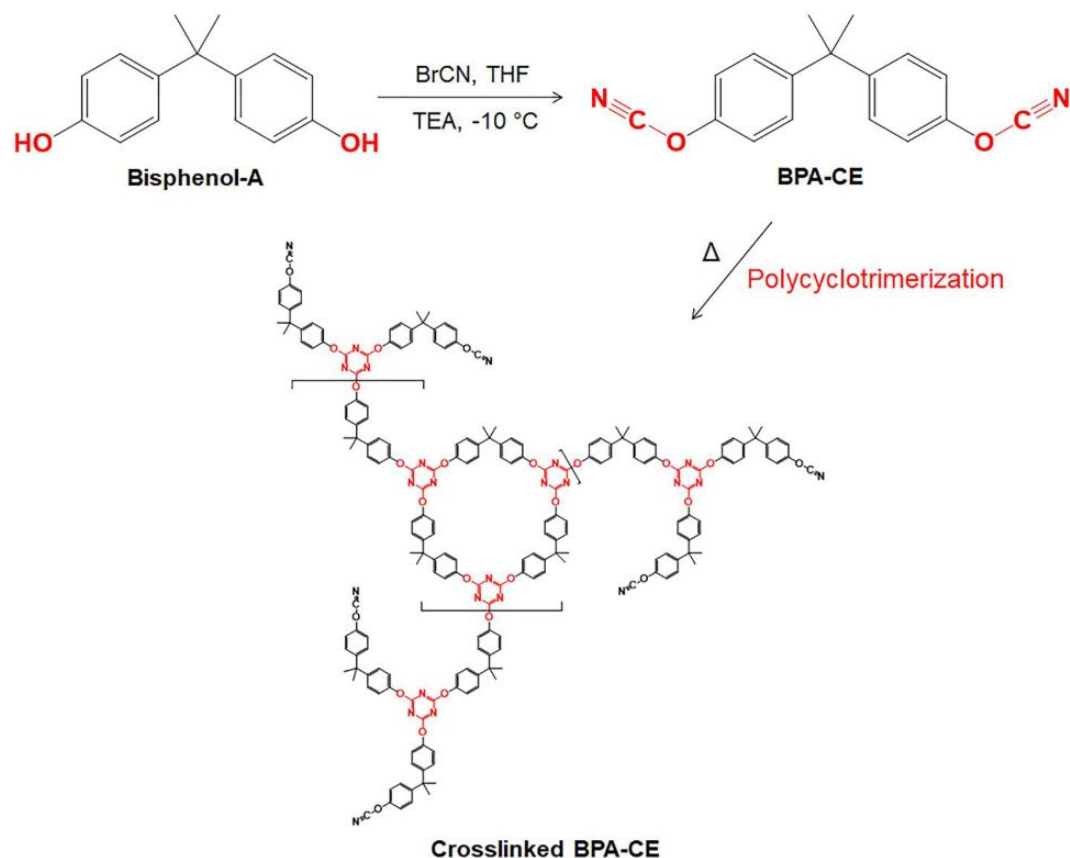


Figure 1. Synthesis of bisphenol-A-based cyanate ester and its cross-linked network.

precursors of cyanate ester resins.² Cyanate ester from bisphenol-A melts at around 79°C, whereas the melting point of cyanate ester from 4,4'-ethylidenebisphenol has been reported to be 29°C.² A slight structural change brings down the melting point for the cyanate esters to be more conveniently processable for the composite applications. Other structural changes are found in the cyanate esters from 4,4'-(hexafluoroisopropylidene)bisphenol (hexafluoro derivative of bisphenol-A) and 4,4'-methylenebis[2,6-xyleneol] (a tetramethyl substituted bisphenol-F), both of which, on curing, display similar glass transition temperatures to cyanate ester from bisphenol-A.² Attempts have been successfully carried out to introduce unsaturated substituents on bisphenol-A cyanate ester. Cross-linked networks of 2,2-bis(3-allyl-4-hydroxyphenyl)propane, a diallyl cyanate ester, have been synthesized, and the glass transition temperature was observed as high as 360°C. Co-cross-linking of diallyl cyanate esters with bismaleimide proved to reduce the brittleness of cross-linked bismaleimide networks.¹⁶ Among other diallyl cyanate esters, bis[[4-[(3-allyl-4-cyanatophenyl)isopropylidene]phenoxy]-phenyl]sulfone and bis[4-(3-allyl-4-cyanatophenoxy)phenyl]sulfone have been synthesized in the past and were used along with bismaleimide resins.¹⁷ Figure 1 displays the synthesis

of bisphenol-A-based cyanate ester and its cross-linked network that possesses triazine rings connecting the bisphenol-A backbone.

However, most of the precursors of cyanate esters are derived from petroleum sources. Petroleum has been the boon for decades, but its limited availability and impacts on the climate change have sought an attention for considering alternate resources. Further, bisphenol-A is identified as a chemical compound with human hazard concerns.¹⁸ Based on the previously mentioned factors, there is a substantial need for replacing bisphenol-A with less toxic and sustainable alternatives. Plant biomass serves as a resource that is both sustainable and less toxic as compared to the petroleum, but it puts forward challenges for successful modifications. Bio-based bisphenolic compounds have been synthesized by several researchers. The condensation of vanillyl alcohol and guaiacol was successfully carried out to synthesize bisguaiacol which was then used for the synthesis of bio-based epoxy resins.¹⁹ Cashew nut shell liquid (derived from cashew nuts) and eugenol (derived from clove) were used to produce renewable bisphenols in the following way. Eugenol and the compounds present in cashew nut shell liquid are phenolic compounds with unsaturated substituents. Isomerizing olefin metathesis was performed to couple them for producing bisphenolic compounds and thus renewable

bisphenols: Dihydroxystilbene derivatives were synthesized.²⁰ In a recent approach, reductive catalytic fractionation of birch wood sawdust was carried out to produce 4-n-propylsyringol, which on further reaction with formaldehyde yielded 3,3⁰-methylenebis(4n-propylsyringol) (m,m⁰-BSF-4P). It was found that m,m⁰BSF-4P is a bisphenolic compound but exhibited lower estrogenic potency than bisphenol-A and can successfully be used to synthesize high-performance aromatic polyesters.²¹ Additionally, the development in the bio-based and especially in the lignin-based monomers, polymers, and high-performance thermoset networks has been documented,^{22–28} but there have been limited studies in the field of cyanate esters. Previous researchers have developed cyanate esters from chemicals obtainable from renewable resources, including resveratrol,²⁹ eugenol,³⁰ carvacrol,³¹ lignin-derived 4-n-propylguaiacol,³² vanillin-based bisphenols,³³ creosol,³⁴ and trans-anethol.^{35,36} All of these cyanate esters possess bifunctionality or trifunctionality; however, they are derived from compounds obtained from biomass resources. Often, it is difficult and economically cumbersome to selectively obtain specific compounds from biomass that often has a complex assembly of natural macromolecules. Thermochemical processes have proved to be efficient in decomposing biomass to simpler organic compounds.³⁷ Fast pyrolysis is a thermochemical process that decomposes biomass to char, gases, and condensable vapors. Condensation of vapors yields a high amount of liquid mixture of hundreds of organic compounds—often called as bio-oil.^{38–40} Fast pyrolysis has been thoroughly studied, and its use for bio-oil production has been critically reviewed.^{39,41–44} Fast pyrolysis is performed to obtain bio-oil from various species of biomass such as pine,^{45–48} switchgrass,^{49,50} corn,⁵¹ bamboo,⁵² forestry residue,^{53,54} agricultural residue,^{55–57} and lignin.^{58–61} Due to its complex compositional nature, extensive characterization has been carried out to study the composition, properties, and aging of the bio-oil.^{62–67} In the present study, the organic phase of bio-oil (ORG-bio-oil) has been utilized as a raw material for monomer synthesis. The ORG-bio-oil is rich in phenolic compounds due to the decomposition of lignin that is a natural, phenolic macromolecule.⁶⁸ Hence, a benefit of pyrolysis is that many biomass species containing lignin can practically be used for obtaining phenolic compounds. In our previous studies, bio-oil has been used for the synthesis of phenol formaldehyde and epoxy polymers.^{69–71} In the present study, we focus on chemical transformation of the mixture of substituted phenols to a mixture of cyanate ester monomers. Further, since most compounds in the bio-oil are monophenolic, it is necessary to introduce bifunctionality or multifunctionality similar to that explained in other bio-based cyanate ester research studies.^{30–}

^{36,72} An approach to synthesize organic biphenol from the bio-oil has also been emphasized in the current work. Depending on the phenolic compounds participating in the reaction, many isomeric biphenolic structures can be obtained, and hence, a mixture of biphenolic monomers can be used as a precursor for further cyanate ester synthesis. The effect of catalysts and reaction conditions on the structure of bisphenols obtained from creosol has been studied earlier.⁷² Our work demonstrates the replacement of bisphenol-A-based cyanate ester by novel, bio-oil-based cyanated monomers as a promising pathway to increase sustainability while maintaining minimum process complexity. In addition, a detailed characterization of bio-oil and the resulting cyanate esters is also outlined.

Experimental section

Materials

Bisphenol-A, chromium(III) acetylacetonate, chloroform-d 99.8p atom% D with 0.03 v/v% trimethylsilane, cyanogen bromide, dichloromethane, ethyl ether stabilized with butylated hydroxytoluene, hydrochloric acid 36.5–38.0%, N-hydroxy-5-norbornene-2,3-dicarboximide (NHND), sodium sulfate anhydrous, tetrahydrofuran, toluene, triethylamine 99%, and 1,3,5-trioxane 98% were ordered from VWR International, Radnor, PA, USA. 2-Chloro-4,4,5,5-tetramethyl-1,3,2-dioxaphospholane (TMDP) was purchased from Sigma-Aldrich, St Louis, Missouri, USA. The ORGbio-oil was obtained from pine wood as per the procedure explained in the “Methods” section.

Methods

Fast pyrolysis of pine

An intermediate-scale auger-fed pyrolysis reactor was used to produce bio-oil from a clean pine wood feedstock (milled to a particle size of less than 4 mm) with a feed rate of 7.3 kg h⁻¹ and a reaction temperature of 500C. The system was purged with N₂ at a flow rate of 50 L min⁻¹.

A detailed instrument description was reported previously.⁷³ The resulting biomass pyrolysis vapors were condensed to yield liquid bio-oil which was further separated into two phases—ORG-bio-oil and aqueous phase. The yield of bio-oil and biochar were measured gravimetrically, and the yield of noncondensable gases was calculated by difference. ORG-bio-oil was characterized by gas chromatography–mass spectrometry (GC-MS), ³¹P-nuclear magnetic resonance (³¹P-NMR) spectroscopy, and Fourier transform infrared (FTIR) spectroscopy, and the density, acid value, water content, and the pH of bio-oils were measured. The bio-oil samples

were stored in a freezer at 10C, and ORG-bio-oil was used for monomer synthesis.

Characterization of ORG-bio-oil

GC-MS was used to measure the chemical composition of the produced ORG-bio-oil. The ORG-bio-oil was dissolved in 99.9% pure MeOH (1 mL bio-oil in 9 mL MeOH), filtered with a polytetrafluoroethylene syringe filter (0.20 mm), and a 1 mL aliquot was injected into the GC-MS system (Clarus 680 gas chromatograph and Clarus SQ 8C mass spectrometer; PerkinElmer, Waltham, Massachusetts, USA). The injection was performed at a split ratio of 80:1 and an injector temperature of 270C. An Elite 1701 MS capillary column (60 m 0.25 mm internal diameter (ID) by 0.25 mm film thickness) with a carrier gas (ultrahighpurity helium, 99.9999%) flow rate of 1 cm³ min⁻¹ and a pressure of 17.3 psi was used. The GC furnace was initially held at 50C for 4 min, then was increased to 280C at 5C min⁻¹, and held at 280C for 5 min. The MS was held at 270C with an ionization energy of 70 eV. Chromatogram peaks were extracted using TurboMass GC-MS software, and the peaks were identified with the National Institute of Standards and Technology Library.

The water content of the ORG-bio-oil was measured by Karl Fischer titration (Metrohm 787 KF Titrino) following the American Society for Testing and Materials protocol (ASTM D4377-00).⁷⁴ The pH of ORG-bio-oil was measured using a pH meter after adding 1 mL of ORGbio-oil into 50 mL of DI water and stirring. The total acid number was measured by dissolving 0.5 g of ORG-bio-oil in 25 mL of 1:1 isopropyl alcohol/water, then titrating with 0.1 N KOH to a pH of 11 in accordance with ASTM D664.⁷⁵ The density of the ORG-bio-oil was determined using a 2 mL glass pycnometer according to ASTM D1475-13.⁷⁶ Analyses were performed in duplicate.

For ³¹P-NMR spectroscopy, bio-oil samples were phosphorylated as per the procedure mentioned in the literature.⁷⁷ NHND and chromium(III) acetylacetonate (20 mg each) were dissolved in the mixture of 3 mL pyridine and 2 mL deuterated chloroform to prepare the stock solution; 550 mL of stock solution was added to around 20 mg of bio-oil sample and stirred well. TMDP (150 mL) was then added to the mixture and stirred well to make the solution homogeneous. The prepared solution was then transferred to the NMR tube, and the spectrum was acquired with a Bruker Avance II 250 MHz spectrometer using inversegated decoupling pulse sequence, 90-degree pulse angle, 25 s pulse delay, and 128 scans. The hydroxyl content of the samples was calculated by integrating relevant peaks compared with the internal standard NHND.

FTIR spectroscopy

FTIR spectroscopy was performed on bio-oil samples and synthesized products using Thermo Scientific Nicolet 6700 FT-IR spectrophotometer (Auburn University, Auburn, AL) equipped with attenuated total reflection accessory and OMNIC 7.3 software. IR spectra were collected in the wavenumber range of 400 cm⁻¹ to 4000 cm⁻¹ at a resolution of 4 cm⁻¹ and 64 scans.

Synthesis of ORG-biphenol

Using GC-MS analysis, it was observed that several monophenolic compounds were present in ORG-bio-oil. ORGbio-oil was dissolved in toluene and washed with water. Toluene and water phases were allowed to separate in a separating funnel overnight. Toluene phase was heated at 80C under vacuum using rotary evaporation to remove toluene, and the resultant, concentrated ORG-bio-oil was treated with 1,3,5-trioxane in acidic conditions to produce biphenolic compounds as per the adapted procedure.³¹ Concentrated ORG-bio-oil and 1,3,5-trioxane (0.3 equiv/OH) were dispersed in water. Concentrated HCl was added to the dispersion in the amount adjusting the normality of reaction mixture at 2.5 N. The reaction mixture was heated at 80C under stirring for 6 h. After cooling down, the reaction mixture was added to dichloromethane and washed with water. The organic phase of the extraction was separated, and dichloromethane was distilled off with rotary evaporation under a reduced pressure and at a room temperature. The synthesis of ORG-biphenol and cyanate esters (described in the next section) is depicted in Figure 2.

ORG-biphenol represents two isomeric categories of compounds differentiated by the position of methylene bridge. This difference is possible due to the reaction mechanism driven by the influence of o,p-directing effects of both the electron-donating groups: OCH₃ and OH substituted on the aromatic rings. The catalyzed synthesis of similar biphenolic compounds and their respective cyanate esters was discussed in the literature.^{32,34,72} Koelewijn et al. found the m,m^o-isomer to be a major product in the mentioned synthesis and o,m^o-isomer having less regioselectivity.³² The ortho-substituted OCH₃ groups have been effective in minimizing the ortho directing effect of OH groups and, hence, lead to m,m^o-coupling effect.³² For the same reason, o,o^o-coupling was observed to be the lowest and considered to be negligible.

Synthesis of cyanate esters

Phenolic monomers ORG-bio-oil, ORG-biphenol, and bisphenol-A were cyanated as per the cyanation procedure^{29,31} to yield various cyanate ester resins. Phenolic monomer was dissolved in tetrahydrofuran in a jacketed,

glass reactor equipped with a mechanical stirrer. The reactor temperature was maintained at 10°C with continuously flowing water/methanol (60:40) mixture through the jacket. After the reaction mixture reached 10°C, cyanogen bromide (1.2 equiv/OH) was added. The mixture was stirred for 5 min, and then dropwise addition of triethylamine was initiated with the help of dropping funnel. The addition of triethylamine was continued for 30 min at 10°C. After the addition process was completed, the cooling was stopped, and the reaction mixture was stirred for 1 h at a room temperature. Tetrahydrofuran was distilled off with rotary

conventional BPA-CE depicted in Figure 1. A continuous triazine network is possible if the cyanate esters bear bifunctionality or multifunctionality, and hence, a similar cross-linked network is expected from ORG-biphenol-CE, with some differences arising from the pendant groups of aromatic rings. ORG-bio-oil-CE, on the other hand, might limit the crosslinking reactions due to monofunctionality.

Cross-linking of cyanate esters

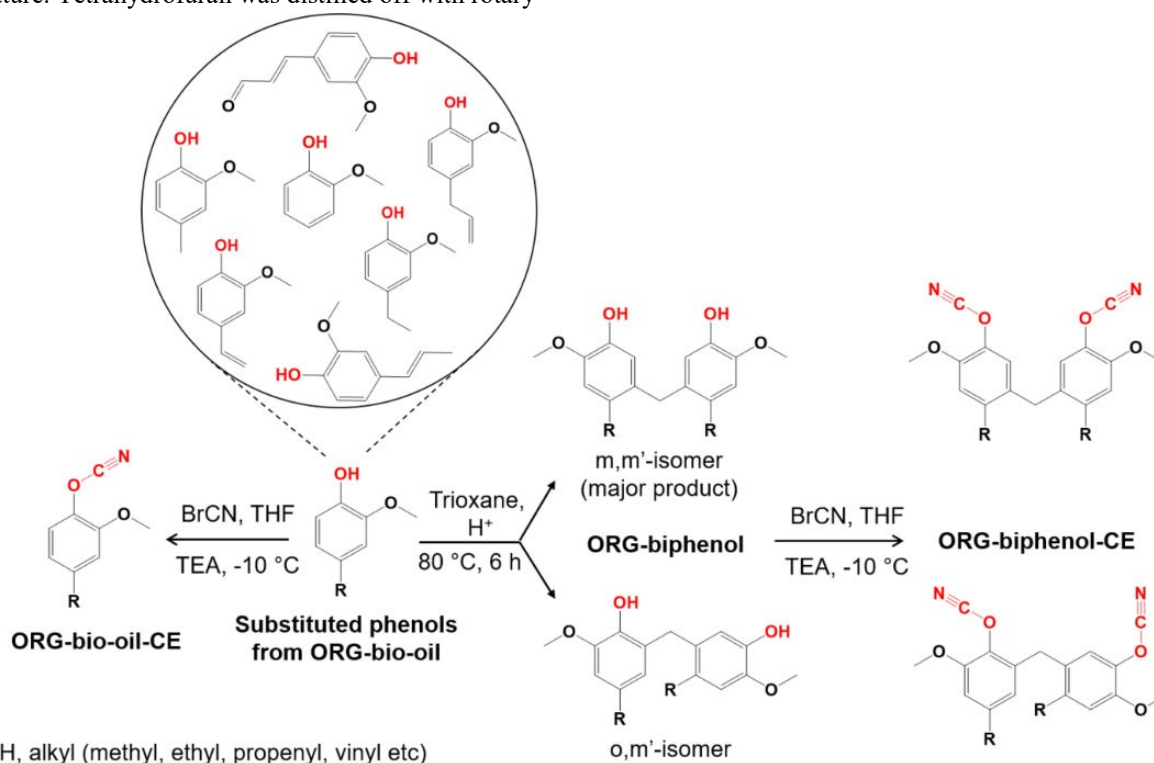


Figure 2. Synthesis of ORG-biphenol, ORG-bio-oil-CE, and ORG-biphenol-CE. ORG-bio-oil-CE: ORG-bio-oil–cyanate ester; ORG-biphenol-CE: ORG-biphenol–cyanate ester.

evaporation. Diethyl ether and water were added to the remaining mixture, and the solution was mixed well and allowed to separate in a separating funnel overnight. The diethyl ether fraction was dried over anhydrous sodium sulfate and filtered, and then, diethyl ether was removed by rotary evaporation under reduced pressure at a room temperature. The cyanate esters from respective monomers were named as ORG-bio-oil-cyanate ester (ORG-bio-oil-CE), ORG-biphenol-cyanate ester (ORG-biphenol-CE), and bisphenol-A-cyanate ester (BPA-CE). Another important aspect for consideration in this study is the cyanate monomer functionality. ORG-bio-oil-CE is predominantly monocyanated mixture because it is derived directly from bio-oil that contains monophenolic compounds, whereas ORG-biphenol-CE provides bifunctionality similar to the

BPA-CE and ORG-bio-oil-CE were blended in different proportions—75:25, 50:50, and 25:75 (by wt%). All the cyanate esters (ORG-bio-oil-CE, ORG-biphenol-CE, BPA-CE, and the blends) were heated at 150°C for 3 h followed by 200°C for 3 h under vacuum. The samples were further postcured at 300°C for 1 h in a conventional furnace. The samples were allowed to cool down and then further used for the thermomechanical analysis.

Differential scanning calorimetry

Differential scanning calorimetry (DSC) was performed by heating uncured sample from the room temperature to 320°C at a heating rate 5°C min⁻¹ under N₂ flow in a TA Instruments Q2000 differential scanning calorimeter, New Castle, DE (available with Auburn University, Auburn, AL) equipped with an autosampler. The heat of

curing and peak curing temperature were observed for the tested samples.

Dynamic mechanical analysis

The cross-linked samples were cut to the dimensions of 30 × 5 × 2 mm³, and the thermomechanical evaluation of polycyanate esters was performed using TA Instruments dynamic mechanical analyzer, RSAIII. An oscillatory stress was applied at 1 Hz frequency on the horizontal specimen using three-point bending geometry to yield a constant 0.1% strain. The temperature was increased at a

Table 1. Properties of ORG-bio-oil.

Fast pyrolysis of pine			
Bio-oil yield (%)	53.7	Bio-char yield (%)	30.4
Noncondensable gas yield (%)			15.9
ORG-bio-oil			
Water content (%)			11.5 ± 0.5
Total acid number (mg KOH/g bio-oil)			100.6 ± 0.0
Density (g/mL)	1.1493 ± 0.0001	pH	3.0 ± 0.2

ORG-bio-oil: organic phase of bio-oil.

rate of 5°C min⁻¹ during the test. The viscoelastic behavior was observed, especially during the glass transition.

Thermogravimetric analysis

Thermogravimetric analysis (TGA) was performed on cyanate ester samples using TA Instruments Q500 thermogravimetric analyzer. Around 10 mg sample was heated from room temperature to 1000°C at a rate of 10°C min⁻¹ under nitrogen purge. Percentage weight loss against temperature and its first derivative were compared for cyanate esters.

Results and discussion

Characterization of ORG-bio-oil, ORG-biphenol, and the cyanate esters

The pyrolysis product yields and the properties of ORGbio-oil are listed in Table 1. ORG-bio-oil was found to be acidic in nature due to its low pH, and it had a low water content. The GC-MS analysis of ORG-bio-oil (Figure 3) revealed major peaks corresponding to substituted phenolic compounds.

The presence of phenolic compounds is likely due to the decomposition of lignin during pyrolysis, which is a polyphenolic macromolecule found in woody

biomass.^{63,78,31} P-NMR spectroscopy (Table 2) yielded quantitative information regarding the hydroxyl number, which was in agreement with the GC-MS results. The amount of phenolic OH was observed to be the maximum among all kinds of OH groups. ORG-biphenol displayed a greater content of phenolic OH, a reduced quantity of acidic OH, and an absence of aliphatic OH as compared to ORG-bio-oil.

In Figure 4(c), the FTIR spectra show that ORGbiphenol displayed a reduction in the peak at 3400–3300 cm⁻¹ corresponding to O–H stretch compared with ORGbio-oil (Figure 4(a)). This agrees with the total hydroxyl number obtained from ³¹P-NMR spectroscopy indicated in Table 2. A slight increase in the intensity of peaks at 2928 cm⁻¹ and 2855 cm⁻¹ relating to sp³ C–H stretch is probably due to a methylene bridge connecting two phenolic moieties in the biphenolic compounds in ORG-biphenol.

Figure 4(b) displays the successful formation of cyanate ester monomers from ORG-bio-oil as evident by the appearance of peaks at 2256 cm⁻¹ and 2201 cm⁻¹ responsible for CN stretch of cyanate ester groups. Another parallel observation of the reduced intensity of the O–H stretch peak in the range of 3400–3300 cm⁻¹ indicated the consumption of hydroxyl groups. Similar changes were observed in the case of ORG-biphenol-CE (appearance of CN stretch at 2260 cm⁻¹ and 2199 cm⁻¹ in Figure 4(d) and reduction in O–H stretch in the range of 3400–3300 cm⁻¹) and BPA-CE (appearance of CN stretch at 2276 cm⁻¹ and 2242 cm⁻¹ in Figure 4(f) and reduction in O–H stretch in the range of 3400–3300 cm⁻¹).

DSC

Table 3 reflects the experimental values for heat of curing and peak curing temperature of uncured cyanate ester samples, and Figure 5 depicts the respective DSC plots. ORGbio-oil-CE displayed the lowest heat of curing and peak curing temperature. Further, it was observed that the addition of ORG-bio-oil-CE brought down the total heat of curing as well as the peak curing temperature of cyanate ester 75:25 blend. The addition of ORG-bio-oil-CE could be beneficial for the processability of blend; however, it could result in low cross-linking as ORG-bio-oil-CE leads to oligomeric cyanate compounds. ORG-biphenol-CE resulted in lower heat of curing and peak curing temperature too indicating better processability. It is possible that the catalyzing effect of unsaturated substituents of the phenolic compounds in bio-oil could have lowered the curing peak temperatures. Similar effect was studied by Koh et al. previously.⁷⁹ Lower heat of curing in comparison with BPA-CE can indicate a more sluggish curing rate. Nonetheless, the assessment of thermal properties of crosslinked ORG-biphenol-CE could present a better picture. As the glass transition region was observed to

be very broad, the values of glass transition temperature were reliably measured from dynamic mechanical analysis (DMA) after 200C, whereas the peak in tan δ was observed at 220C in Figure 6(b).

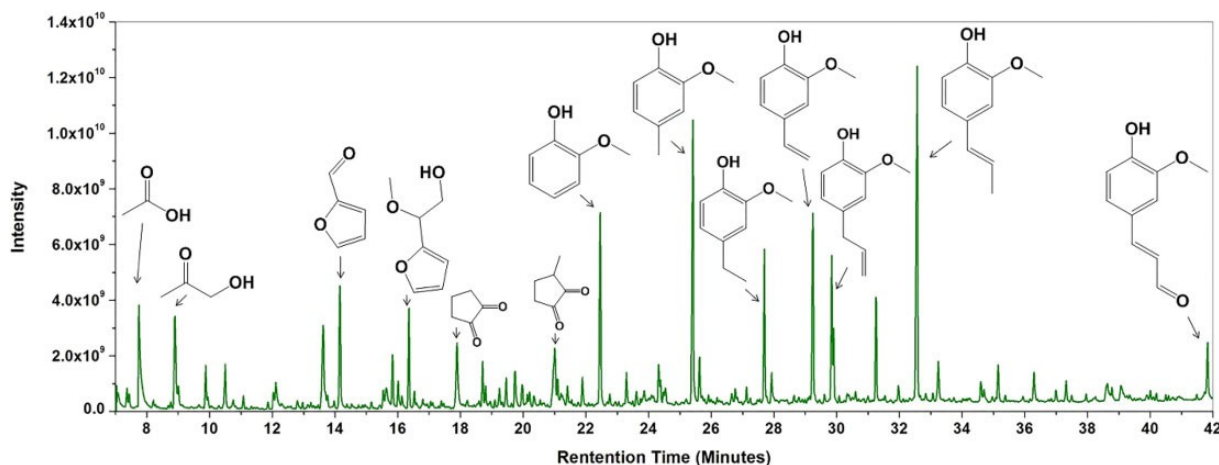


Figure 3. GC-MS analysis of ORG-bio-oil. GC-MS: gas chromatography–mass spectroscopy; ORG-bio-oil: organic phase of bio-oil.

Table 2. ^{31}P -NMR spectroscopy of ORG-bio-oil and ORG-biphenol.

OH type	Range (ppm)	OH content (mmol OH/g sample)		
		ORG-bio-oil	ORG-biphenol	
Aliphatic OH	150–145.5	1.57	0	
Phenolic OH	C-5 substituted condensed phenolic OH	-5	0.07	0.23
	Guaiacyl phenolic OH	4-O-5	0.10	0.24
	Catechol type OH	5-5	0.28	0.27
	p-Hydroxyphenyl OH	141.7–140.2	0.27	2.35
	140.2–139.0	1.45	2.89 (54%)	1.27 (89%)
	139.0–138.2	0.60		0.30
	138.2–137.3	0.39		0.05
Acidic OH	136.6–133.6	0.84		0.29
Total		5.30		2.64

^{31}P -NMR: ^{31}P -nuclear magnetic resonance; ORG-bio-oil: organic phase of bio-oil. discussed in the further section.

Thermomechanical performance of cyanate esters

The DMA of ORG-bio-oil-CE and ORG-biphenol-CE yielded good thermomechanical properties in comparison with BPA-CE, yet considerable viscoelastic differences. In Figure 6(a), cross-linked BPA-CE was observed to have a high storage modulus at a room temperature, with a value of 3 GPa. The BPA-CE sample showed an onset of glass transition at 190C and a sharp decrease in storage modulus

The cross-linked blend of BPA-CE/ORG-bio-oil-CE (75:25) displayed a similar behavior, with an onset glass transition temperature at 128C and the peak in tan δ at 175C. Other blends of BPA-CE and ORG-bio-oil-CE (50:50 and 25:75) were too brittle to be analyzed with DMA and did not withstand the applied cyclic stress. It was earlier found in other studies that cyanate ester polymers possess brittleness, and hence, the attempts have been made for toughening the cyanate esters.⁸⁰ As ORG-bio-oil-CE is a mixture of monocyanate esters, a higher amount of ORG-bio-oil-CE limits the polycyclotrimerization leading to oligocyanate solid product rather than a cross-linked cyanate network and, hence, resulting in brittle samples. The reduction in the cross-

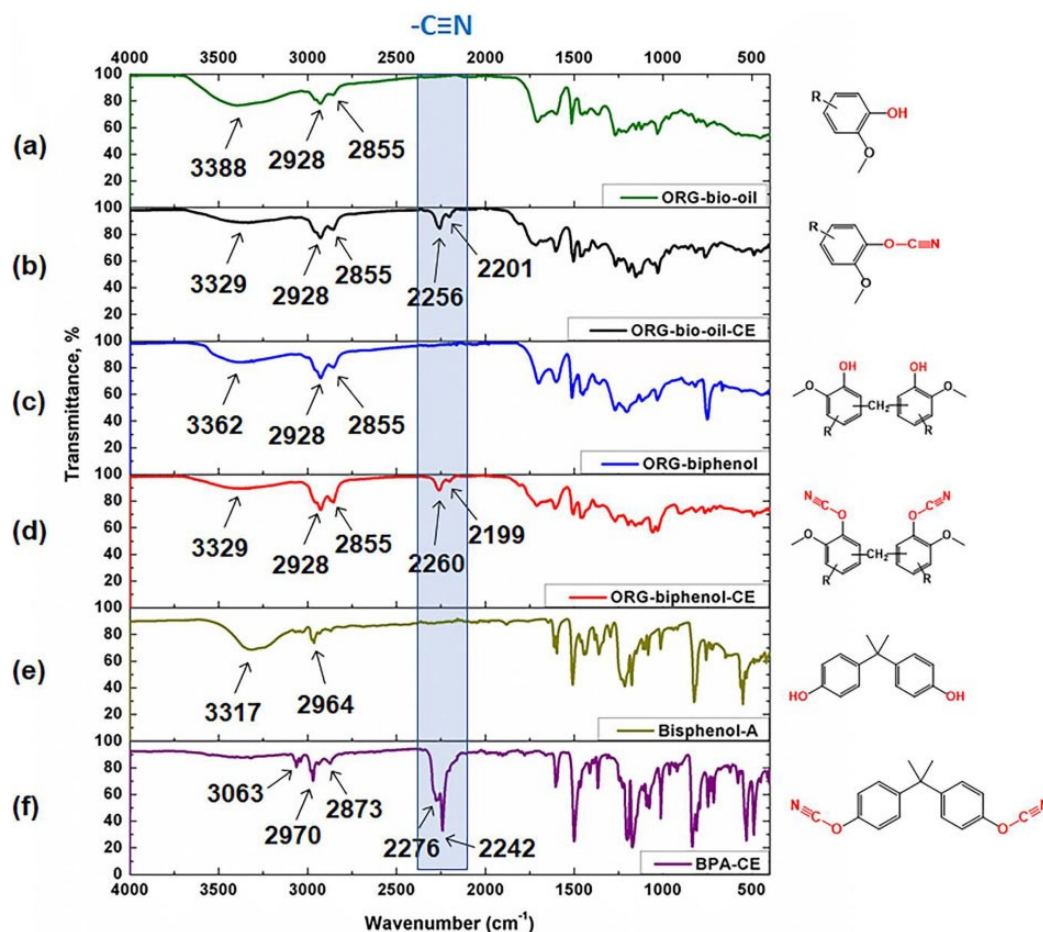


Figure 4. FTIR spectra of (a) ORG-bio-oil, (b) ORG-bio-oil-CE, (c) ORG-biphenol, (d) ORG-biphenol-CE, (e) bisphenol-A, and (f) BPA-CE. FTIR: Fourier transform infrared; ORG-bio-oil: organic phase of bio-oil; ORG-bio-oil-CE: ORG-bio-oil–cyanate ester; ORG-biphenol-CE: ORG-biphenol–cyanate ester; BPA-CE: bisphenol-A–cyanate ester.

link density of cured network can lead to decrease in glass transition temperature and overall thermomechanical performance.^{81–83} In the case of BPA-CE and the 75:25 blend, a small plateau of storage modulus was observed after the glass transition region. Cross-linked ORG-biphenol-CE was characterized by a lower storage modulus (around 0.3 GPa) at a room temperature and a gradual decline in the storage modulus over a wide range of temperature. An onset temperature was observed at 354C, and the maximum value of tan was found to be at 378C. Glass transition temperatures were also considered based on the loss modulus peak for comparison and have been listed in Table 4.

Cross-linked ORG-biphenol-CE can be considered a material with cross-links formed by triazine rings due to cyanate bifunctionality. Moreover, ORG-biphenol possessed a substituent group on the aromatic rings due to the presence of substituted phenols in ORG-bio-oil. The substituted groups could restrict the molecular mobility of the network, resulting in superior glass transition temperature as compared to BPA-CE which lacks phenolic ring substituents. A combination of triazine

network and the possible formation of additional covalent bonds resulting from the substituents of the aromatic rings is expected to occur in the case of cross-linked ORG-biphenol-CE, which might facilitate thermal transitions over a very broad range and, hence, the resulting behavior of the storage modulus observed in Figure 6(a). A broad tan peak is observed in the case of the cross-linked ORG-biphenol-CE sample (Figure 6(b)), which supports this argument. It can be said that the glass transition temperature of cross-linked ORG-biphenol-CE lies in the range of 350–380C. In the case of BPA-CE/

Table 3. Differential scanning calorimetry of uncured cyanate esters.

Sample	Heat of curing, H_c (J g ⁻¹)	Peak curing temperature, T_c (C)
BPA-CE	543.7	212.93
ORG-biphenol-CE	266.3	160.79
ORG-bio-oil-CE	74.7	140.71

BPA-CE/ORG-bio-oilCE 421.2 199.78
 (75:25 blend)

BPA-CE: bisphenol-A-cyanate ester; ORG-biphenol-CE: ORG-biphenol-cyanate ester; ORG-bio-oil: organic phase of bio-oil; ORG-bio-oil-CE: ORG-bio-oil-cyanate ester.

ORG-bio-oil-CE-75:25 sample, ORG-bio-oil-CE reduced the cross-linking density due to the monofunctionality of ORG-bio-oil-CE and hence reduced the glass transition temperature range for the blend. Monocyanated esters limit the polymerization, thereby producing materials with less or negligible cross-linking. ORG-bio-oil also contains aliphatic hydroxyl compounds that, on cyanation, yield

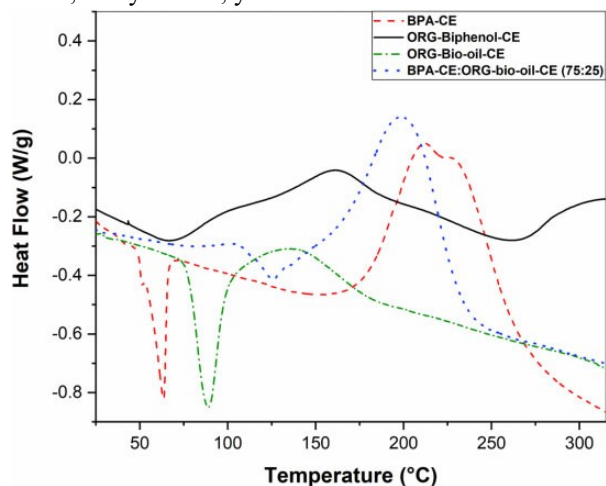


Figure 5. Thermal analysis of cyanate esters.

aliphatic cyanate esters. Aliphatic cyanate esters rearrange to aliphatic isocyanates that can react with water or moisture to produce carbamate derivatives. These products

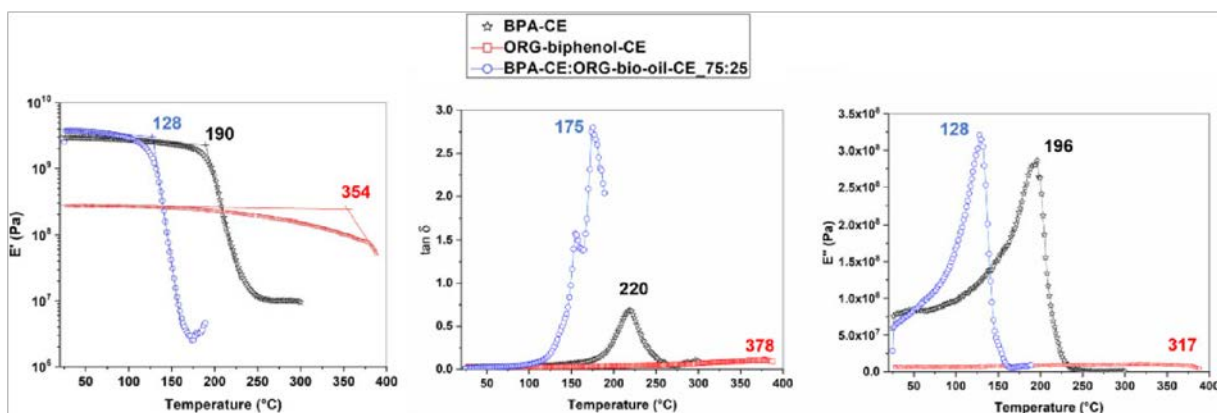


Figure 6. Thermomechanical properties of cyanate esters: (a) storage modulus, (b) tan , and (c) loss modulus.

Table 4. Thermomechanical properties of cyanate esters.

Sample	Glass transition temperature (C)			Storage modulus (GPa)	
	Onset storage modulus	Tan peak	Loss modulus peak	At room temperature (glassy region)	Active chains density (mol m ³)
BPA-CE	190	220	196	2.96	734
ORG-biphenol-CE	354	378	317	0.27	3093
BPA-CE/ORG-bio-oil-CE (75:25)	128	175	128	3.75	227

BPA-CE: bisphenol-A–cyanate ester; ORG-biphenol-CE: ORG-biphenol–cyanate ester; ORG-bio-oil: organic phase of bio-oil; ORG-bio-oil-CE: ORGbio-oil–cyanate ester.

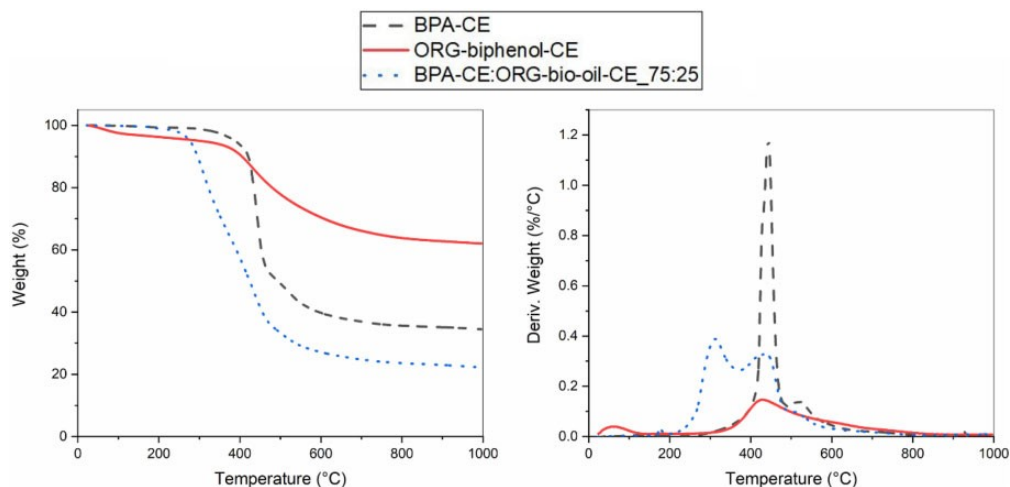


Figure 7. Thermogravimetric analysis cyanate esters.

hinder cross-linking at elevated temperatures. A similar phenomenon of a reduction in the glass transition temperature by monofunctional cyanate esters has been previously studied by other researchers.⁸⁴ Moreover, a probable heterogeneity leading to a phase separation between two different cyanate esters in the BPA-CE/ORG-bio-oilCE_75:25 sample led to two maxima in tan curve (Figure 6(b)). The cross-linking extent or the cross-link density of the

cyanate ester sample was compared by calculating active chains density. The active chains density (n) of a sample was calculated as follows:

$$n \frac{1}{4} E^0 = 3RT$$

where E⁰ is the storage modulus at temperature T after the glass transition region and R is the universal gas constant (8.314 J (mol.K)⁻¹). The equation is based on the ideal rubber theory and derived from the relationship between

shear and storage moduli considering the Poisson's ratio for rubber to be approximately 0.5.⁸⁵ The active chains density was observed to be far more for ORG-biphenol-CE as compared to BPA-CE and ORG-bio-oil-CE. This is mainly due to the high value of storage modulus observed after the glass transition in the case of ORG-biphenol-CE.

TGA

Figure 7 contains the TGA plots of percentage weight loss with temperature for cured cyanate esters.

BPA-CE and ORG-biphenol-CE were found to possess similar thermal stability. Both the samples displayed thermal degradation after 400C. The peak degradation temperature for BPA-CE was observed at 444C and for ORG-biphenol-CE at 426C. ORG-biphenol-CE retained more mass after 1000C (62%) compared with BPA-CE (34.5%). This can be related to a possible higher carbon content in the case of ORG-biphenol-CE due to the bio-oil fractions derived from lignin pyrolysis. Blend BPA-CE/ ORG-bio-oil-CE exhibited lowest mass retention (22.2%) after 1000C and also displayed a first peak degradation temperature at 312C and second peak at 436C. It is imperative that ORG-bio-oil-CE is more thermally degradable than ORG-biphenol-CE and BPA-CE.

Conclusions

Lignocellulosic biomass, such as wood, can be utilized as feedstock for chemicals using fast pyrolysis. The ORG-biooil contains a mixture of substituted phenolic compounds along with other organics as the decomposition products of fast pyrolysis process. Bio-oil-derived phenolic hydroxyl compounds offer an opportunity for cyanation, which leads to the synthesis of bio-oil-based cyanate ester monomers. Nonetheless, ORG-bio-oil contains monophenolic compounds that produce monocyanated esters on direct cyanation. Monofunctional cyanate esters yield materials with less glass transition temperature. ORG-bio-oil can be successfully used to synthesize ORG-biphenol that resembles the structure of bisphenol-A, a traditional petrochemicalbased monomer for cyanate ester synthesis. ORG-biphenol has a higher phenolic OH content as well as an absence of aliphatic hydroxyl compounds as compared to ORG-biooil. The FTIR spectroscopy confirms the synthesis of cyanate ester resins. The DSC confirmed the lowering of peak curing temperature of bio-oil-based cyanate esters. Further, the thermal stability of bio-oil-based cyanate esters was similar to BPA-CE, and an improved mass retention after 1000C was found in the case of ORG-biphenol-CE. Crosslinked cyanate ester

from ORG-biphenol yielded a higher glass transition temperature than that of cross-linked cyanate esters derived from bisphenol-A and also displayed a superior active chains density. The present study was successful in preparing sustainable cyanate esters from bio-oil (ORG-bio-oil-CE and ORG-biphenol-CE), and 25 wt% of replacement of BPA-CE was possible by the direct cyanation of ORG-bio-oil. It can be concluded that cyanate ester resins can be developed from the bio-oil pyrolyzed from complex lignocellulosic biomass and have the potential to be used in the applications of polymer composites.

Acknowledgements

The authors would like to acknowledge US Department of Agriculture–National Institute of Food and Agriculture, National Science Foundation Center of Excellence in Nanobiomaterials (NSF-CREST) derived from biorenewable and waste resources, and NSF-CREST Center for Sustainable Lightweight Materials for funding this study.


Declaration of conflicting interests

The author(s) declared no potential conflicts of interest with respect to the research, authorship, and/or publication of this article.

Funding

The author(s) disclosed receipt of the following financial support for the research, authorship, and/or publication of this article: This work was financially supported by US Department of Agriculture–National Institute of Food and Agriculture (USDA-NIFA2015-67021-22842), National Science Foundation Center of Excellence in Nanobiomaterials (NSF-CREST) derived from biorenewable and waste resources, and NSF-CREST Center for Sustainable Lightweight Materials award #1735971.

ORCID iD

Maria Lujan Aua  <https://orcid.org/0000-0001-6932-5645>

References

1. Kessler MR. Cyanate ester resins. In: Nicolais L and Borzacchiello A (eds) Wiley Encyclopedia of Composites. 2nd ed. Hoboken: John Wiley & Sons, 2012, pp. 658–672.
2. Nair CPR, Mathew D and Ninan KN. Cyanate ester resins, recent developments. *Adv Polym Sci* 2001; 155: 1–99.
3. Fang T and Shimp DA. Polycyanate esters – science and applications. *Prog Polym Sci* 1995; 20: 61–118. DOI: 10.1016/0079-6700(94)e0006-m.
4. Wang G, Fu G, Gao TL, et al. Preparation and characterization of novel film adhesives based on cyanate ester resin for

- bonding advanced radome. *Int J Adhes Adhes* 2016; 68: 80–86. DOI: 10.1016/j.ijadhadh.2016.02.004.
5. Inamdar A, Cherukattu J, Anand A, et al. Thermoplastictoughened high-temperature cyanate esters and their application in advanced composites. *Ind Eng Chem Res* 2018; 57: 4479–4504. DOI: 10.1021/acs.iecr.7b05202.
 6. Toldy A, Szlancsik A and Szolnoki B. Reactive flame retardancy of cyanate ester/epoxy resin blends and their carbon fibre reinforced composites. *Polym Degrad Stabil* 2016; 128: 29–38. DOI: 10.1016/j.polymdegradstab.2016.02.015.
 7. Zhan GZ, Zhao L, Hu S, et al. A novel biobased resin epoxidized soybean oil modified cyanate ester. *Polym Eng Sci* 2008; 48: 1322–1328. DOI: 10.1002/pen.21096.
 8. Lei YX, Xu MZ, Jiang ML, et al. Curing behaviors of cyanate ester/epoxy copolymers and their dielectric properties. *High Perform Polym* 2017; 29: 1175–1184. DOI: 10.1177/0954008316672291.
 9. Zegaoui A, Wang AR, Dayo AQ, et al. Effects of gamma irradiation on the mechanical and thermal properties of cyanate ester/benzoxazine resin. *Radiat Phys Chem* 2017; 141: 110–117. DOI: 10.1016/j.radphyschem.2017.06.010.
 10. Kumar KSS, Nair CPR and Ninan KN. Investigations on the cure chemistry and polymer properties of benzoxazine cyanate ester blends. *Eur Polym J* 2009; 45: 494–502. DOI: 10.1016/j.eurpolymj.2008.11.001.
 11. Wang YQ, Wu GL, Kou KC, et al. Mechanical, thermal conductive and dielectrical properties of organic montmorillonite reinforced benzoxazine/cyanate ester copolymer for electronic packaging. *J Mater Sci Mater El* 2016; 27: 8279–8287. DOI: 10.1007/s10854-016-4834-5.
 12. Ohashi S, Kilbane J, Heyl T, et al. Synthesis and characterization of cyanate ester functional benzoxazine and its polymer. *Macromolecules* 2015; 48: 8412–8417. DOI: 10.1021/acs.macromol.5b02285.
 13. Wan L, Zhang X, Wu GL, et al. Thermal conductivity and dielectric properties of bismaleimide/cyanate ester copolymer. *High Voltage* 2017; 2: 167–171. DOI: 10.1049/hve.2017.0056.
 14. Hamerton I. High-performance thermoset-thermoset polymer blends: a review of the chemistry of cyanate ester bismaleimide blends. *High Perform Polym* 1996; 8: 83–95. DOI: 10.1088/0954-0083/8/1/006.
 15. Iredale RJ, Ward C and Hamerton I. Modern advances in bismaleimide resin technology: a 21st century perspective on the chemistry of addition polyimides. *Prog Polym Sci* 2017; 69: 1–21. DOI: 10.1016/j.progpolymsci.2016.12.002.
 16. Barton JM, Hamerton I and Jones JR. A study of the thermal and dynamic mechanical-properties of functionalized aryl cyanate esters and their polymers. *Polym Int* 1993; 31: 95–106. DOI: 10.1002/pi.4990310114.
 17. Chaplin A, Hamerton I, Howlin BJ, et al. Development of novel functionalized aryl cyanate ester oligomers. 1. Synthesis and thermal characterization of the monomers. *Macromolecules* 1994; 27: 4927–4935. DOI: 10.1021/ma00096a013.
 18. Ng FF, Couture G, Philippe C, et al. Bio-based aromatic epoxy monomers for thermoset materials. *Molecules* 2017; 22: 48. DOI: 10.3390/molecules22010149.
 19. Hernandez ED, Bassett AW, Sadler JM, et al. Synthesis and characterization of bio-based epoxy resins derived from vanillyl alcohol. *ACS Sustainable Chem Eng* 2016; 4: 4328–4339. DOI: 10.1021/acssuschemeng.6b00835.
 20. Trita AS, Over LC, Pollini J, et al. Synthesis of potential bisphenol A substitutes by isomerising metathesis of renewable raw materials. *Green Chem* 2017; 19: 3051–3060. DOI: 10.1039/c7gc00553a.
 21. Koelewijn SF, Cooreman C, Renders T, et al. Promising bulk production of a potentially benign bisphenol A replacement from a hardwood lignin platform. *Green Chem* 2018; 20: 1050–1058. DOI: 10.1039/c7gc02989f.
 22. Llevot A, Grau E, Carlotti S, et al. From lignin-derived aromatic compounds to novel biobased polymers. *Macromol Rapid Comm* 2016; 37: 9–28. DOI: 10.1002/marc.201500474.
 23. Raquez JM, Deleglise M, Lacrampe MF, et al. Thermosetting (bio)materials derived from renewable resources: a critical review. *Prog Polym Sci* 2010; 35: 487–509. DOI: 10.1016/j.progpolymsci.2010.01.001.
 24. Jiang Y, Ding DC, Zhao S, et al. Renewable thermoset polymers based on lignin and carbohydrate derived monomers. *Green Chem* 2018; 20: 1131–1138. DOI: 10.1039/c7gc03552g.
 25. Zhao S, Huang XN, Whelton AJ, et al. Formaldehyde-free method for incorporating lignin into epoxy thermosets. *ACS Sustainable Chem* 2018; 6: 10628–10636. DOI: 10.1021/acssuschemeng.8b01962.
 26. Fache M, Boutevin B and Caillol S. Epoxy thermosets from model mixtures of the lignin-to-vanillin process. *Green Chem* 2016; 18: 712–725. DOI: 10.1039/c5gc01070e.
 27. Stanzione JF, Giangiulio PA, Sadler JM, et al. Lignin-based bio-oil mimic as biobased resin for composite applications. *ACS Sustainable Chem* 2013; 1: 419–426. DOI: 10.1021/sc3001492.
 28. Stanzione JF, Sadler JM, La Scala JJ, et al. Lignin model compounds as bio-based reactive diluents for liquid molding resins. *ChemSusChem* 2012; 5: 1291–1297. DOI: 10.1002/cssc.201100687.
 29. Cambrea LR, Davis MC, Garrison MD, et al. Processable cyanate ester resin from cis resveratrol. *J Polym Sci Pol Chem* 2017; 55: 971–980. DOI: 10.1002/pola.28457.
 30. Harvey BG, Guenther AJ, Yandek GR, et al. Synthesis and characterization of a renewable cyanate

- ester/polycarbonate network derived from eugenol. *Polymer* 2014; 55: 5073–5079. DOI: 10.1016/j.polymer.2014.08.034.
31. Harvey BG, Guenther AJ, Koontz TA, et al. Sustainable hydrophobic thermosetting resins and polycarbonates from turpentine. *Green Chem* 2016; 18: 2416–2423. DOI: 10.1039/c5gc02893k.
32. Koelewijn SF, Van den Bosch S, Renders T, et al. Sustainable bisphenols from renewable softwood lignin feedstock for polycarbonates and cyanate ester resins. *Green Chem* 2017; 19: 2561–2570. DOI: 10.1039/c7gc00776k.
33. Harvey BG, Guenther AJ, Meylemans HA, et al. Renewable thermosetting resins and thermoplastics from vanillin. *Green Chem* 2015; 17: 1249–1258. DOI: 10.1039/c4gc01825g.
34. Meylemans HA, Harvey BG, Reams JT, et al. Synthesis, characterization, and cure chemistry of renewable bis(cyanate) esters derived from 2-methoxy-4-methylphenol. *Biomacromolecules* 2013; 14: 771–780. DOI: 10.1021/bm3018438.
35. Davis MC, Guenther AJ, Sahagun CM, et al. Polycyanurate networks from dehydroanethole cyclotrimers: synthesis and characterization. *Polymer* 2013; 54: 6902–6909. DOI: 10.1016/j.polymer.2013.10.050.
36. Davis MC, Guenther AJ, Groshens TJ, et al. Polycyanurate networks from anethole dimers: synthesis and characterization. *J Polym Sci Pol Chem* 2012; 50: 4127–4136. DOI: 10.1002/pola.26218.
37. Kamm B, Gerhardt M and Leiß S. The biorefinery concept – thermochemical production of building blocks and syngas. In: Crocker M (ed) *Thermochemical Conversion of Biomass to Liquid Fuels and Chemicals*. Cambridge: Royal Society of Chemistry, 2010, pp. 46–62.
38. Bridgwater AV, Meier D and Radlein D. An overview of fast pyrolysis of biomass. *Org Geochem* 1999; 30: 1479–1493. DOI: 10.1016/s0146-6380(99)00120-5.
39. Mohan D, Pittman CU and Steele PH. Pyrolysis of wood/biomass for bio-oil: a critical review. *Energ Fuel* 2006; 20: 848–889. DOI: 10.1021/ef0502397.
40. Bridgwater AV. Review of fast pyrolysis of biomass and product upgrading. *Biomass Bioenerg* 2012; 38: 68–94. DOI: 10.1016/j.biombioe.2011.01.048.
41. Kan T, Strezov V and Evans TJ. Lignocellulosic biomass pyrolysis: a review of product properties and effects of pyrolysis parameters. *Renew Sust Energ Rev* 2016; 57: 1126–1140. DOI: 10.1016/j.rser.2015.12.185.
42. Shen DK, Jin W, Hu J, et al. An overview on fast pyrolysis of the main constituents in lignocellulosic biomass to value-added chemicals: structures, pathways and interactions. *Renew Sust Energ Rev* 2015; 51: 761–774. DOI: 10.1016/j.rser.2015.06.054.
43. Rahman MM, Liu RH and Cai JM. Catalytic fast pyrolysis of biomass over zeolites for high quality bio-oil – a review. *Fuel Process Technol* 2018; 180: 32–46. DOI: 10.1016/j.fuproc.2018.08.002.
44. Mostafazadeh AK, Solomatnikova O, Drogui P, et al. A review of recent research and developments in fast pyrolysis and bio-oil upgrading. *Biomass Conversion and Biorefinery* 2018; 8: 739–773. DOI: 10.1007/s13399-018-0320-z.
45. Westerhof RJM, Brillman DWF, Garcia-Perez M, et al. Stepwise fast pyrolysis of pine wood. *Energ Fuel* 2012; 26: 7263–7273. DOI: 10.1021/ef301319t.
46. Yildiz G, Lathouwers T, Toraman HE, et al. Catalytic fast pyrolysis of pine wood: effect of successive catalyst regeneration. *Energ Fuel* 2014; 28: 4560–4572. DOI: 10.1021/ef500636c.
47. Wang JX, Cao JP, Zhao XY, et al. Study on pine sawdust pyrolysis behavior by fast pyrolysis under inert and reductive atmospheres. *J Anal Appl Pyrol* 2017; 125: 279–288. DOI: 10.1016/j.jaap.2017.03.015.
48. Thangalazhy-Gopakumar S, Adhikari S, Ravindran H, et al. Physicochemical properties of bio-oil produced at various temperatures from pine wood using an auger reactor. *Bioresour Technol* 2010; 101: 8389–8395. DOI: 10.1016/j.biortech.2010.05.040.
49. Mullen CA and Boateng AA. Chemical composition of bio-oils produced by fast pyrolysis of two energy crops. *Energ Fuel* 2008; 22: 2104–2109. DOI: 10.1021/ef700776w.
50. Serapiglia MJ, Mullen CA, Boateng AA, et al. Impact of harvest time and cultivar on conversion of switchgrass to bio-oils via fast pyrolysis. *Bioenerg Res* 2017; 10: 388–399. DOI: 10.1007/s12155-016-9812-5.
51. Mullen CA, Boateng AA, Goldberg NM, et al. Bio-oil and bio-char production from corn cobs and stover by fast pyrolysis. *Biomass Bioenerg* 2010; 34: 67–74. DOI: 10.1016/j.biombioe.2009.09.012.
52. Wang J, Zhong ZP, Ding K, et al. Catalytic fast pyrolysis of bamboo sawdust via a two-step bench scale bubbling fluidized bed/fixed bed reactor: study on synergistic effect of alkali metal oxides and HZSM-5. *Energ Convers Manage* 2018; 176: 287–298. DOI: 10.1016/j.enconman.2018.09.029.
53. Oasmaa A, Kuoppala E, Gust S, et al. Fast pyrolysis of forestry residue. 1. Effect of extractives on phase separation of pyrolysis liquids. *Energ Fuel* 2003; 17: 1–12. DOI: 10.1021/ef020088x.
54. Oasmaa A, Kuoppala E and Solantausta Y. Fast pyrolysis of forestry residue. 2. Physicochemical composition of product liquid. *Energ Fuel* 2003; 17: 433–443. DOI: 10.1021/ef020206g.

55. Oasmaa A, Solantausta Y, Arpiainen V, et al. Fast pyrolysis bio-oils from wood and agricultural residues. *Energy Fuels* 2010; 24: 1380–1388. DOI: 10.1021/ef901107f.
56. Yanik J, Kommayer C, Saglam M, et al. Fast pyrolysis of agricultural wastes: characterization of pyrolysis products. *Fuel Process Technol* 2007; 88: 942–947. DOI: 10.1016/j.fuproc.2007.05.002.
57. Wang YP, Zeng ZH, Tian XJ, et al. Production of bio-oil from agricultural waste by using a continuous fast microwave pyrolysis system. *Bioresource Technol* 2018; 269: 162–168. DOI: 10.1016/j.biortech.2018.08.067.
58. Wang SR, Wang KG, Liu Q, et al. Comparison of the pyrolysis behavior of lignins from different tree species. *Biotechnol Adv* 2009; 27: 562–567. DOI: 10.1016/j.biotechadv.2009.04.010.
59. Bai XL, Kim KH, Brown RC, et al. Formation of phenolic oligomers during fast pyrolysis of lignin. *Fuel* 2014; 128: 170–179. DOI: 10.1016/j.fuel.2014.03.013.
60. Shen D, Zhao J, Xiao R, et al. Production of aromatic monomers from catalytic pyrolysis of black-liquor lignin. *J Anal Appl Pyrol* 2015; 111: 47–54. DOI: 10.1016/j.jaap.2014.12.013.
61. Fan LL, Zhang YN, Liu SY, et al. Bio-oil from fast pyrolysis of lignin: effects of process and upgrading parameters. *Bioresource Technol* 2017; 241: 1118–1126. DOI: 10.1016/j.biortech.2017.05.129.
62. Stas M, Kubicka D, Chudoba J, et al. Overview of analytical methods used for chemical characterization of pyrolysis biooil. *Energy Fuels* 2014; 28: 385–402. DOI: 10.1021/ef402047y.
63. Kanaujia PK, Sharma YK, Garg MO, et al. Review of analytical strategies in the production and upgrading of bio-oils derived from lignocellulosic biomass. *J Anal Appl Pyrol* 2014; 105: 55–74. DOI: 10.1016/j.jaap.2013.10.004.
64. Mullen CA and Boateng AA. Characterization of water insoluble solids isolated from various biomass fast pyrolysis oils. *J Anal Appl Pyrol* 2011; 90: 197–203. DOI: 10.1016/j.jaap.2010.12.004.
65. Andersson T, Hyotylainen T and Riekkola ML. Analysis of phenols in pyrolysis oils by gel permeation chromatography and multidimensional liquid chromatography. *J Chromatogr A* 2000; 896: 343–349. DOI: 10.1016/S0021-9673(00)00678-6.
66. Michailof CM, Kalogiannis KG, Sfetsas T, et al. Advanced analytical techniques for bio-oil characterization. *Wires Energy Environ* 2016; 5: 614–639. DOI: 10.1002/wene.208.
67. Hao N, Ben HX, Yoo CG, et al. Review of NMR characterization of pyrolysis oils. *Energy Fuels* 2016; 30: 6863–6880. DOI: 10.1021/acs.energyfuels.6b01002.
68. Jacobson K, Maheria KC and Dalai AK. Bio-oil valorization: a review. *Renew Sust Energy Rev* 2013; 23: 91–106. DOI: 10.1016/j.rser.2013.02.036.
69. Barde M, Adhikari S, Via BK, et al. Synthesis and characterization of epoxy resins from fast pyrolysis bio-oil. *Green Materials* 2018; 6: 76–84.
70. Celikbag Y, Meadows S, Barde M, et al. Synthesis and characterization of bio-oil-based self-curing epoxy resin. *Ind Eng Chem Res* 2017; 56: 9389–9400. DOI: 10.1021/acs.iecr.7b02123.
71. Sibaja B, Adhikari S, Celikbag Y, et al. Fast pyrolysis bio-oil as precursor of thermosetting epoxy resins. *Polym Eng Sci* 2018; 58: 1296–1307.
72. Meylemans HA, Groshens TJ and Harvey BG. Synthesis of renewable bisphenols from creosol. *ChemSusChem* 2012; 5: 206–210. DOI: 10.1002/cssc.201100402.
73. Kim P, Weaver S, Noh K, et al. Characteristics of bio-oils produced by an intermediate semipilot scale pyrolysis auger reactor equipped with multistage condensers. *Energy Fuels* 2014; 28: 6966–6973. DOI: 10.1021/ef5016186.
74. ASTM D4377-00. Standard test method for water in crude oils by potentiometric Karl Fischer titration. ASTM International: West Conshohocken, PA, 2011: 1–7.
75. ASTM D664-11a. Standard test method for acid number of petroleum products by potentiometric titration. ASTM International: West Conshohocken, PA, 2011: 1–11.
76. ASTM D1475-13. Standard test method for density of liquid coatings, inks, and related products. ASTM International: West Conshohocken, PA, 2011: 1–4.
77. Ben HX and Ragauskas AJ. NMR characterization of pyrolysis oils from kraft lignin. *Energy Fuels* 2011; 25: 2322–2332. DOI: 10.1021/ef2001162.
78. Sipila K, Kuoppala E, Fagernas L, et al. Characterization of biomass-based flash pyrolysis oils. *Biomass Bioenergy* 1998; 14: 103–113. DOI: 10.1016/S0961-9534(97)10024-1.
79. Koh HCY, Dai J, Tan E, et al. Catalytic effect of 2,2'-diallyl bisphenol A on thermal curing of cyanate esters. *J Appl Polym Sci* 2006; 101: 1775–1786. DOI: 10.1002/app.23533.
80. Kinloch AJ and Taylor AC. The toughening of cyanate-ester polymers – Part II – chemical modification. *J Mater Sci* 2003; 38: 65–79. DOI: 10.1023/a:1021109731672.
81. Georjon O and Galy J. Effects of crosslink density on mechanical properties of high class transition temperature polycyanurate networks. *J Appl Polym Sci* 1997; 65: 2471–2479. DOI: 10.1002/(sici)1097-4628(19970919)65:12<2471::aid-app18>3.0.co;2-3.
82. Goertzen WK and Kessler MR. Thermal and mechanical evaluation of cyanate ester composites with low-temperature

- processability. *Compos Part A Appl S* 2007; 38: 779–784. DOI: 10.1016/j.compositesa.2006.09.005.
83. Zhao S and Abu-Omar MM. Renewable epoxy networks derived from lignin-based monomers: effect of crosslinking density. *ACS Sustainable Chem* 2016; 4: 6082–6089. DOI: 10.1021/acssuschemeng.6b01446.
84. Papatomas KI and Wang DW. Triazine networks modified with monofunctional reactive cyanate ester monomers. *J Appl Polym Sci* 1992; 44: 1267–1274. DOI: 10.1002/app.1992.070440716.
85. Sperling LH. Cross-linked polymers and rubber elasticity. In: Sperling LH (ed) *Introduction to Physical Polymer Science*. Hoboken: John Wiley & Sons, 2006, pp. 445–448.